Scientific Research Publishing

Open Journal of Applied Sciences, 2023, 13, 1910-1934
https://www.scirp.org/journal/ojapps
ISSN Online: 2165-3925
ISSN Print: 2165-3917

Thermal Properties of Earth Bricks Stabilised with Cement and Sawdust Residue Using the Asymmetrical Hot-Plane Method

Gabin Alex Nouemssi[1*#], Guy Edgar Ntamack[2*], Martin Ndibi Mbozo'O[3*], Bonaventure Djeumako[3*]

[1]Ecole Nationale Supérieure des Sciences Agros Industrielles Laboratoire de Mécanique, Matériaux et Photonique, University of Ngaoundéré, Ngaoundéré, Cameroon
[2]Département de Physique/EGCIM, Faculté des Sciences et Physique, Université de Ngaoundéré, Ngaoundéré, Cameroon
[3]Ecole Nationale Supérieure des Sciences Agros Industrielles, Département de Génie Mécanique et Productique, University of Ngaoundéré, Ngaoundéré, Cameroon
Email: #gabinnouemssi@gmail.com, guyedgar@yahoo.fr, martinpaulndibi185@yahoo.fr, djeumakobona@yahoo.fr

How to cite this paper: Nouemssi, G.A., Ntamack, G.E., Mbozo'O, M.N. and Djeumako, B. (2023) Thermal Properties of Earth Bricks Stabilised with Cement and Sawdust Residue Using the Asymmetrical Hot-Plane Method. *Open Journal of Applied Sciences*, **13**, 1910-1934.
https://doi.org/10.4236/ojapps.2023.1311151

Received: October 2, 2023
Accepted: November 13, 2023
Published: November 16, 2023

Abstract

This paper presents an experimental study of the characterisation of local materials used in the construction and thermal insulation of buildings. These materials are compressed earth bricks stabilised with cement and sawdust. The thermal conductivity, diffusivity, effusivity, and specific heat of earth-based materials containing cement or sawdust have been determined. The results show that the blocks with earth + sawdust are better thermal insulators than the blocks with simple earth. We observe an improvement in thermal efficiency depending on the presence of sawdust or cement stabilisers. For cement stabilisation, the thermal conductivity increases (λ: 1.04 to 1.36 $W \cdot m^{-1} \cdot K^{-1}$), the diffusivity increases (from 4.32×10^{-7} to 9.82×10^{-7} $m^2 \cdot s^{-1}$), and the effusivity decreases (1404 - 1096 $J \cdot m^{-2} \cdot K^{-1} \cdot s^{-1/2}$). For sawdust stabilisation, the thermal conductivity decreases (λ: 1.04 to 0.64 $W \cdot m^{-1} \cdot K^{-1}$), the diffusivity increases (from 4.32×10^{-7} to 5.9×10^{-7} $m^2 \cdot s^{-1}$), and the effusivity decreases (1404 - 906 $J \cdot m^{-2} \cdot K^{-1} \cdot s^{-1/2}$). Improving the structural and thermal efficiency of BTC via stabilisation with derived binders or cement is beneficial for the load-bearing capacity and thermal performance of buildings.

Keywords

Clay Brick, West Cameroon, Thermal Conductivity, Asymmetric Hot Surface, Thermal Properties

*These authors contributed equally to this work.
#Corresponding author.

1. Introduction

Earth is a building material that is not only ecological, but also cheap and available. It also seems to be one of the oldest building materials, along with pebbles. In order to master earth construction, several authors have carried out studies on the properties of earth blocks intended for the construction of buildings and dwellings. Studies on compacted stabilised earth blocks have been carried out by several researchers [1]-[10]. Authors [1] [2] [3] [4] discuss cement stabilisation and analyse the effect of cement on the hydromechanical properties of materials. Refs. [5] [6] [7] discuss plant fibre stabilisation, hydromechanical properties and thermal properties of clay blocks. Ref. [8] tries to find the relationship between the shape of the building and the thermal behaviour of the building. Ref. [9] analyses the effect of air movement on building behaviour. Ref. [10] evaluates the performance of the building in response to the use of household appliances.

The development of bio-based materials contributes to improving the living conditions of the population. Despite its advantages in terms of mechanical properties and durability, the stabilisation of earth raw materials using cement or sawdust has several natural advantages: low energy and carbon footprint, recyclability, moisture exchange capacity and hygrothermal performance [10] [11] [12]. Stabilisation of raw soils can also be achieved by mechanical compaction at relatively low to high pressures (2 to 10 MPa) [13] or by hyper-compaction up to 100 MPa [14]. However, hyper-compaction requires high quality equipment and energy to achieve such compaction pressures. Therefore, attempts have also been made to stabilise the soil by physically incorporating granular particles such as sand and agricultural aggregates or residues [15] [16]. Compaction and/or incorporation of granules or fibres can affect mechanical and/or thermal performance due to their physico-mechanical effects in the soil matrix. In order to reduce the energy consumption of a building, it is essential to favour, from the design stage, systems that are integrated into the structure and provide natural thermal and hygroscopic comfort, thus reducing the need for conventional energy. Thermal insulation is an effective way of compensating for losses in the building envelope, since a large proportion of heat loss occurs through the vertical walls. The use of insulating building materials can reduce heat transfer through building walls [17]. In recent years, bio-based materials have been developed that meet both the technical criteria usually required of conventional building materials and the environmental criteria over their lifetime [17]. For example, composites based on bamboo or black coconut fibres have been used for thermal insulation while maintaining suitable mechanical properties [17].

Some studies have already attempted to stabilise BTC using binders. The authors of [18] stabilised BTCs using rice husk ash (RHA), a pozzolan produced by calcining a by-product from rice fields, as a partial replacement for lime. This method improved the compressive strength and reduced the water absorption of BECs. In [19], coal fly ash, lime and wood aggregates were used to produce earth blocks. In [20], the stabilising effect of the combination of lime and natural poz-

zolan and steam curing up to 75˚C on the performance of BECs was evaluated. Steam curing accelerated the pozzolanic reaction to achieve optimum compressive strength within 24 h, while the natural pozzolan improved other mechanical and durability properties of the earth blocks. A recent study [21] showed that soil mixes with residual calcium carbide produce earth bricks with good mechanical performance. Ref. [22] investigated the effect of bamboo fibre length and content on the physico-mechanical and hygroscopic properties of compressed earth blocks (CEBs) used in construction. Ref. [23] evaluated the effect of cement on the physico-mechanical and hygroscopic properties of Compressed Earth Blocks (CEB) used in the construction of the city of Ngaoundéré.

Earth bricks are widely used in Cameroon. Their thermophysical properties are still poorly understood. Our experimental study focused on local Cameroonian materials, earth and sawdust, where the earth is stabilised with a small amount of cement and/or natural sawdust. The thermal properties of the materials studied were measured during tests on specimens prepared in the laboratory. The results obtained make it possible to formulate hypotheses on the optimal use of these materials.

2. Material Characteristics

Earth-block buildings can be found all over the world. In Burkina Faso, for example, we have the primary school of Gado (**Figure 1**), and in Cameroon, we have the task of promoting local materials for earth buildings (**Figure 2**). The quality of these buildings depends on the formulation of their materials (**Figure 3**). In our work, the materials used to make the three types of earth bricks are simple earth, earth + cement, and earth + sawdust.

2.1. Earth

Clay samples should be taken at depths of −30 cm and −50 cm to avoid sampling the organic part of the soil (**Figure 4**). For our study, we needed samples from Bangangté town, specifically from the entrance to the town in a mud brick production area (**Figure 5**).

Figure 1. Gado primary school, Burkina Faso.

Figure 2. MIPROMALO Cameroon.

Figure 3. Erosion and cracking of unstabilised mud-brick walls exposed to rain. West Cameroon.

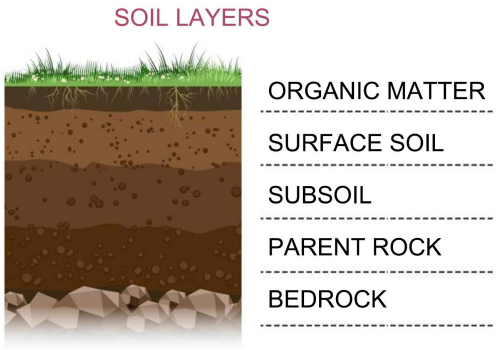

Figure 4. Soil layers.

Figure 5. Production area for blocks of unstabilised earth (adobe). West Cameroon.

2.2. Preparation of the Land for Manufacturing

After removing the soil, leave it in the sun for a few days to dry at room temperature. 24 hours before making the test pieces, place them in an oven set at room temperature to maximise drying.

2.3. Cement

The robust cement used, from the Cameroon Cement Works (CIMENCAM), is of the Portland grey type with additives (pozzolan or limestone), with the characteristics prescribed by the Cameroonian standard for hydraulic binders. It corresponds to the cement type CEM II B-P 42.5R. Cement, a hydraulic binder, is suitable for soils with low clay content or low plasticity and for soils with low-activity clays. During its hydration with the water contained in the soil, cement is transformed over time into stable, water-resistant crystals that form bonds between the grains of the soil. This reaction requires a sufficient amount of water. Furthermore, as the cement reaches its hardness and maximum strength in 28 days (the time required for the cement to set well in the material), the blocks must remain wet during this period. They are covered with a plastic sheet, or if this is not possible, they are watered. In their work, the authors of [8] show an increase in compressive strength with increasing cement content in the material.

2.4. Sawdust

The tree known locally as padauk (**Figure 6**) belongs to the Papilionaceae family (Leguminosae, Papilionoideae, Fabaceae) and has the scientific name Pterocarpus soyauxii. It is located in the equatorial forests of Nigeria up to the Central African Republic, as well as the Democratic Republic of Congo and Angola. Pterocarpus soyauxii is distributed from Cameroon to the Democratic Republic of Congo. This tree is a substantial species found in the tropical forest, with a straight, cylindrical trunk that can grow up to 15 - 20 metres in height and regularly exceeds 1.50 metres in diameter. Its sapwood, which is 10 cm thick, is white in colour, and it is clearly distinct from the heartwood, which has a blood-red colour. The colour changes to purplish-brown in the presence of air. A perfect

Figure 6. Padauk Sawdust.

wood demonstrates good resistance against weathering agents and is thus classified as durable. As with all sapwood, padauk sapwood is less resistant to attack by wood-wetting agents than heartwood. Padauk is a semi-heavy wood with an average density of 770 kg/m^3. It is highly stable and has high hygroscopicity. Padauk exhibits low mechanical strength. The analysis of the chemical composition by the Center Technique Forest-ier Tropical (C. T. F. T.) revealed the following: alcohol-benzene extractables at a rate of 12.00%, water at 1.37%, pentosans at approximately 10.95%, cellulose at 41.85%, and lignin at 30.55%. Due to its durability, padauk is suitable for interior carpentry such as stairs, floors, and notably truck-bed floors. It can also be used for building structures, frames, canoes, and exterior carpentry such as windows and doors. The wood's colour is valued for carving, furniture, cabinets, knife and tool handles, combs, walking sticks, and musical instruments (C. T. F. T., 1978). The reddish colour of the heartwood makes it a source of dye for the textile industry. This dye is used to give a red colour to fabrics and clothes. The wood contains high levels of tannins, which facilitate mordanting during fibre dyeing. In 1980, the C. T. F. T. conducted a study on the ethereal extract and identified the following compounds: homopterocarpine, pterostilbene, prunetine (a dihydroxy-4',5,methoxy-7 isoflavone), and sandalwood (a trihydroxy4',5,5,7-methoxy isoflavone).

2.5. Preparation of Sawdust

After collecting the sawdust without a sawmill, allow it to dry at room temperature for a week before using.

3. Experimental and Numerical Methods for Thermal Characterisation Using the Asymmetric Hot-Plane Method

3.1. Experimental Measurement Device Description

The asymmetrical hot-plane method (Figure 7) is advantageous due to its simplicity, precision, speed, and ease of implementation. This method enables the

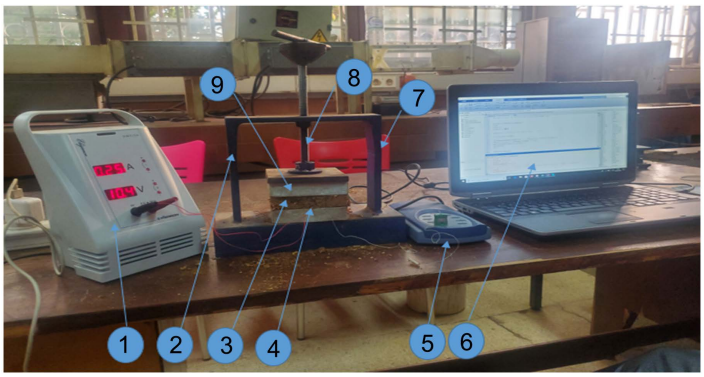

Figure 7. This is a photo of the asymmetrical hot plate measurement device in use, along with the measurement chain. The measurements were taken with the following equipment numbered as follows: 1—Stabilised power supply; 2—Gauges; 3—Sample; 4—Hot plate (the space between the sample and the polystyrene); 5—Temperature recorder; 6—Computer; 7—Additional gauges; 8—Clamping device; 9—Polystyrene foam.

estimation of both thermal conductivity and effusivity [24]. In comparison to other methods, such as the hot-disk method or the hot-wire method (which is not suitable for lightweight materials), it requires little financial investment. This method will be used for our studies, as it provides both technological and financial benefits.

3.2. Principle of the Method

- The method's principle involves applying a constant heat flow step ($\varphi = 0$ for $t < t_0$ and $\varphi = \varphi_0$ for $t > t_0$) to the heating resistor. The temperature evolution of Ts(t) is recorded in the centre of this resistor, where a thermocouple is in place. While the disturbance has not affected the other faces, and assuming the semi-infinite medium hypothesis is valid (*i.e.*, while $T_e(t)$ remains constant), we assume the transfer in the centre of the sample to be unidirectional. Modelling this heat transfer enables the calculation of the temperature evolution in the centre of the sample (**Figure 8**). The values of the following are calculated by applying the following parameter-estimation method.
- The thermal effusivity, E, can be calculated using the formula $E = \sqrt{\lambda \rho c}$, where λ represents the thermal conductivity of the material, ρ represents the density of the material, and c represents the specific heat capacity of the material.
- The thermal capacitance $(mc)_s$ of the probe and assembly of the heating resistor.
- The contact resistance R_c at the interface between the probe and the sample should be minimised to reduce the difference between the theoretical and experimental T_s (t) curves.
- Modelling of the semi-infinite heated plane (**Figure 9**).

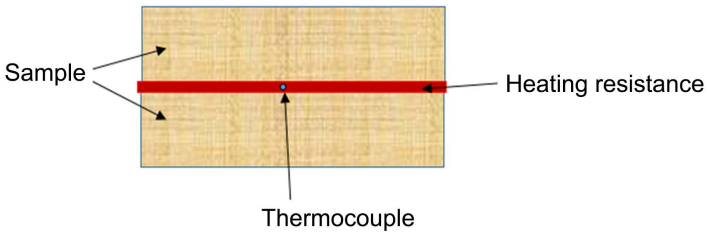

Figure 8. Hot-plane method assembly diagram.

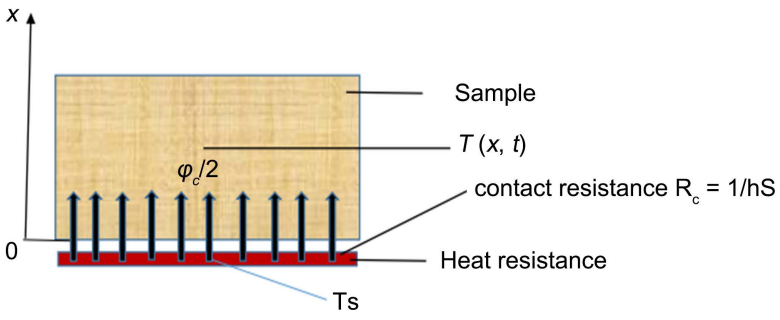

Figure 9. Modelling of the semi-infinite heated plane.

In a hot-plane device, an electric resistor with small thickness, mass (m_s), and heat capacity (C_s) is placed between two samples of the material to be characterised. The resistor is subjected to a density of heat flow Φ and has a supposedly uniform temperature T_s.

The sample demonstrates the heat equation:

$$\frac{\partial^2 T}{\partial x^2} = \frac{1}{a}\frac{\partial T}{\partial t} \tag{1}$$

Consider the following boundary conditions:

$$\begin{cases} T(x,0) = T_s(0) = T_i & (2) \\ T(\infty,t) = T_i & (3) \\ h\left[T_s(t) - T(0,t) = -\lambda \dfrac{\partial T(0,t)}{\partial x}\right] & (4) \\ \dfrac{\varnothing_0 S}{2} = m_s c_s \dfrac{\mathrm{d}T_s}{\mathrm{d}t} + hS\left[T_s(t) - T(0,t)\right] & (5) \end{cases}$$

Relation (1) expresses the conservation of heat flux at the surface of the semi-infinite medium, while relation (2) expresses the conservation of heat flux at the level of electrical resistance.

The variable is changed as follows: $\overline{T} = T - T_i$ from $\frac{\partial \overline{T}}{\partial X} = \frac{\partial T}{\partial X}$, $\frac{\partial^2 \overline{T}}{\partial X} = \frac{\partial^2 T}{\partial X}$ et $\frac{\partial \overline{T}}{\partial t} = \frac{\partial T}{\partial t}$.

We can express Equation (1) as follows:

$$\frac{\partial^2 \overline{T}}{\partial X^2} = \frac{1}{\alpha}\frac{\partial \overline{T}}{\partial t} \tag{6}$$

$$\begin{cases} \overline{T}(x,0) = 0 & (7) \\ \overline{T}(\infty,t) = 0 & (8) \\ h\left[\overline{T}_s(t) - \overline{T}(0,t) = -\lambda \dfrac{\partial \overline{T}(0,t)}{\partial x}\right] & (9) \\ \dfrac{\varnothing_0 S}{2} = m_s c_s \dfrac{\mathrm{d}\overline{T}_s}{2\mathrm{d}t} + hS\left[\overline{T}_s(t) - \overline{T}(0,t)\right] & (10) \end{cases}$$

$$\theta(X,p) = A\mathrm{e}^{-qx}; \quad A = \theta(0,p).$$

$$\theta_s(p) = \frac{\varnothing_0 S}{2P}\frac{1 + R_C ES\sqrt{P}}{\dfrac{m_s c_s}{2}p + \left[R_C \dfrac{m_s c_s}{2}P + 1\right]ES\sqrt{P}}$$

Equations (4) and (5) are transformed into Laplace space as follows:

$$\begin{cases} h\left[\theta_s(p) - \theta(0,p)\right] = -\lambda \dfrac{\partial \theta(0,p)}{\partial x} = \sqrt[\lambda]{\dfrac{P}{a}}\theta(0,p) = E\sqrt{P}\theta & (11) \\ \dfrac{\theta_0 S}{2P} = \dfrac{m_s c_s}{2}p\theta(p) + hs\left[\theta_s(p) - \theta(0,p)\right] & (12) \end{cases}$$

$$\theta_s(p) = \frac{\varnothing_0 S}{2P}\frac{1 + R_C ES\sqrt{P}}{\dfrac{m_s c_s}{2}p + \left[R_C \dfrac{m_s c_s}{2}P + 1\right]ES\sqrt{P}} \tag{13}$$

$$\varnothing_s(p)=\frac{\varnothing_0 S}{2}\frac{1+R_c ES\sqrt{p}}{\left(\frac{mc}{2}\right)_s p+ES\sqrt{p}} \tag{14}$$
$$=\frac{\varnothing_0}{2Ep^{3/2}}\left(1+R_C ES\sqrt{p}\right)\left[1-\frac{(mc)_s}{2ES}\sqrt{p}\right]$$

$$\theta_s(p)=\frac{\varnothing_0}{2Ep^{3/2}}\left[1+\left(R_C ES\sqrt{p}-\frac{(mc)_s}{2ES}\right)\sqrt{p}\right] \tag{15}$$
$$=\frac{\varnothing_0}{2Ep^{3/2}}+\frac{\varnothing_0}{2}\left(R_C-\frac{(mc)_s}{2ES}\right)$$

$$T_s(t)-T_s(0)=\varnothing_0 S\left(R_c-\frac{(mc)_s}{2ES}\right)+\frac{\varnothing_0}{E\sqrt{\pi}}\sqrt{t} \tag{16}$$

Plotting $T_s(t)-T_s(0)$ against $\sqrt{t}$ results in a straight line with a slope of $\frac{\varnothing_0}{E\sqrt{\pi}}$, which can be used to determine the thermal effusivity *E*. The temperature is not affected by the probe's inertia or the contact resistance over a significant duration. The assumption of a semi-infinite medium must be valid for the chosen estimation interval to apply this estimation method.

Complete 1D model

Heat transfer in a solid that is opaque, homogeneous, and isotropic can be mathematically represented using the heat equation

$$\frac{1}{a}\frac{\partial T}{\partial t}=\nabla^2 T \tag{17}$$

The parameter "*a*" represents the thermal diffusivity and is a function of λ and ρcP.

The system is modelled with the assumption that the heat transfer remains unidirectional towards the centre of the device throughout the measurement period. The hypothesis is verified through a 1D simulation on COMSOL and an analysis of the estimation residuals, which are the differences between the temperature obtained through the 1D model $T_{mod}(t)$ and the experimental temperature $T_{exp}(t)$.

Based on these assumptions, we can express the following.

- By considering the heat flux density $\varnothing_{01}$ leaving the probe towards the sample.

$$\begin{bmatrix}\theta\\ \varnothing_{01}\end{bmatrix}=\begin{bmatrix}1 & 0\\ C_{hp} & 1\end{bmatrix}\begin{bmatrix}1 & R_c\\ 0 & 1\end{bmatrix}\begin{bmatrix}A & B\\ C & D\end{bmatrix}\begin{bmatrix}A_i & B_i\\ C_i & D_i\end{bmatrix}\begin{bmatrix}0\\ \varnothing_1\end{bmatrix}=\begin{bmatrix}A_1 & B_1\\ C_1 & D_1\end{bmatrix}\begin{bmatrix}0\\ \varnothing_1\end{bmatrix} \tag{18}$$

$$\varnothing_{01}=\theta_1\frac{D_1}{B_1} \tag{19}$$

$$\begin{bmatrix}\theta\\ \varnothing_{02}\end{bmatrix}=\begin{bmatrix}A_i & B_i\\ C_i & D_i\end{bmatrix}\begin{bmatrix}0\\ \varnothing_2\end{bmatrix} \tag{20}$$

$$\varnothing_{02}=\theta\frac{D_i}{B_i} \tag{21}$$

$$\varnothing_0 = \varnothing_{01} + \varnothing_{02} = \frac{\varnothing_0}{S} \tag{22}$$

$$A = D = \cosh(qe);\quad B = \frac{\sinh(qe)}{\lambda q};\quad C = \lambda q \sin(qe);\ \text{avec}\quad q = \sqrt{\frac{p}{a}} \tag{23}$$

$$A_i = D_i = \text{coshi}(q_i e_i);\quad B_i = \frac{\sinh(q_i e_i)}{\lambda_i q_i};\quad C_i = \lambda_i q_i \sinh(q_i e_i)$$

$$q_i = \sqrt{\frac{p}{a_i}} \tag{24}$$

λ: The thermal conductivity of the sample.

a: The thermal diffusivity of the sample.

e: The thickness of the sample.

λ_i: The thermal conductivity of polystyrene.

a_i: The thermal diffusivity of polystyrene.

e_i: The thickness of the polystyrene.

$$\theta(p) = \frac{\varnothing_0(p)}{\frac{D_1}{B_1} + \frac{D_i}{B_i}} \tag{25}$$

θ: The Laplace transform of $T(t)$.

$\varnothing_{01}$: The Laplace transform of the flux dissipated towards the sample.

$\varnothing_{02}$: The Laplace transform of the heat flux dissipated towards the polystyrene.

$\varnothing_0$: The Laplace transform of the total heat flux produced by the heating element.

φ_0: The total heat flux produced by the heating element.

C_h: The heat capacity of the heating element per unit area: $C_h = \rho_h c_h e_h$.

R_c: The contact resistance between the heating element and the sample.

$\varnothing_1$: The Laplace transform of the flux density transmitted to the upper aluminium block.

$\varnothing_2$: The Laplace transform of the flux density transmitted to the lower aluminium block Simplified model.

Simplified model

At the beginning of the heating process, the sample behaves as a semi-infinite medium. The temperature at the centre of the heated surface confirms this statement.

$$\theta(p) = \frac{\varnothing_0(p)}{E_i\sqrt{p} + \frac{C_{hp} + \left(1 + R_c C_{hp}\right) E\sqrt{p}}{1 + R_c E\sqrt{p}}} \tag{26}$$

For sufficiently long times ($p \to 0$) and considering a flux step, $\varnothing_0(p) = \frac{\varphi_0}{p}$ limited development, which leads to:

$$\theta(p) \approx \frac{\varphi_0}{p^{3/2}(E+E_i)} + \frac{\varphi_0 R_c E^2 - C_h}{p(E+E_i)^2} \tag{27}$$

The thermal effusivity can be estimated from the slope α of the linear segment of the curve using inverse Laplace transformation.

$(t) = (\sqrt{t})$ with:

$$E = \frac{\varphi_0}{\alpha\sqrt{\pi}} - E_i \tag{28}$$

Furthermore, assuming a semi-stationary regime at longer times enables us to express

$$\varnothing = \left[\rho ce + (\rho ce)_i - (\rho ce)_s\right]\frac{\mathrm{d}T}{\mathrm{d}t} \tag{29}$$

The heat capacity ρc can be estimated from the slope β of the curve $T(t)$ using the following relationship:

$$\rho c = \frac{\varnothing}{\beta} - (\rho ce)_i - (\rho ce)_s \tag{30}$$

3.3. Manufacture of Specimens

The experimental equipment (**Figure 10**) for producing test specimens comprises the metal mould, along with its accessories and the hydraulic press. The mould is constructed using an 8 mm thick steel sheet designed specifically to resist deformation under compaction pressure. While the openings on the lid and the bottom of the mould enable the filling of the mould, they also permit the unmoulding of the specimen after compaction. The sliding action of two metal plates inside the mould enables the flattening of the specimen surfaces.

Figure 10. Mould and the hydraulic press used for the manufacture of the specimens.

- Sieving

The soil has been double-sifted in order to retain only particles with a grain size with a diameter between 4 mm and 12.5 mm. This grain size makes it possible to eliminate the fine particles that are not sufficiently porous. In fact, the presence of pores (filled with air) in the soil aggregates helps to reduce the thermal conductivity of the material and makes it a better thermal insulator [25]. Furthermore, the mechanical resistance increases with the fineness of the soil due to the reduction in the volume of air. A granulometry of diameters between 4 mm and 12.5 mm was chosen to find a compromise between good thermal insulation and acceptable mechanical resistance [25].

The grain size of the soil used is less than 12.5 mm.

- Preparation of the mix to be compacted (**Figure 11**)
- After the materials have dried, and to carry out the compaction, water is added to the mixture of cement and laterite until the desired consistency is reached. The amount of water needed to obtain this consistency is 13% of the total mass (**Table 1**).

Figure 11. A 10 × 10 × 3 specimen.

Table 1. Composition of the specimens.

Designation	Earth (%)	Water (%)	Cement (%)	Sawdust (%)
BTC 0	87	13	0	0
BTC C4	83	13	4	0
BTC C6	81	13	6	0
BTC C8	79	13	8	0
BTC Sp4	83	13	0	4
BTC Sp6	81	13	0	6
BTC Sp8	79	13	0	8

4. Result and Discussion

4.1. Thermal Conductivity

Evolution of the parameters with the stabilizer (Conductivity, Table 2 and Figure 12).

4.2. Effusivity

Evolution of the parameters with the stabilizer (Effusively, Figure 13).

4.3. Diffusivity

Evolution of the parameters with the stabilizer (Diffusivity, Figure 14).

4.4. Heat Capacity

Evolution of the parameters with the stabilizer (Heat capacity, Figure 15).

Table 2. Thermal conductivity results.

Thermal Conductivity				
Test Tube	Content Stabilising %	Thickness (cm) Earth Block	Thermal Conductivity with Cement λ (W/m/K)	Thermal Conductivity Sawdust λ (W/m/K)
BTC 0	0	3	1.02	1.02
BTC 0	0	3	0.98	0.98
BTC 0	0	3	1.09	1.09
BTC 0	0	3	1.07	1.07
Mean			1.04	1.04
BTC 4	4	3	1.18	0.87
BTC 4	4	3	1.29	0.80
BTC 4	4	3	1.02	1.02
BTC 4	4	3	1.55	0.73
Mean			1.26	0.85
BTC 6	6	3	1.21	0.70
BTC 6	6	3	1.15	0.80
BTC 6	6	3	1.05	0.77
BTC 6	6	3	1.67	0.73
Mean			1.27	0.75
BTC 8	8	3	1.18	0.67
BTC 8	8	3	1.38	0.70
BTC 8	8	3	1.26	0.63
BTC 8	8	3	1.62	0.56
Mean			1.36	0.64

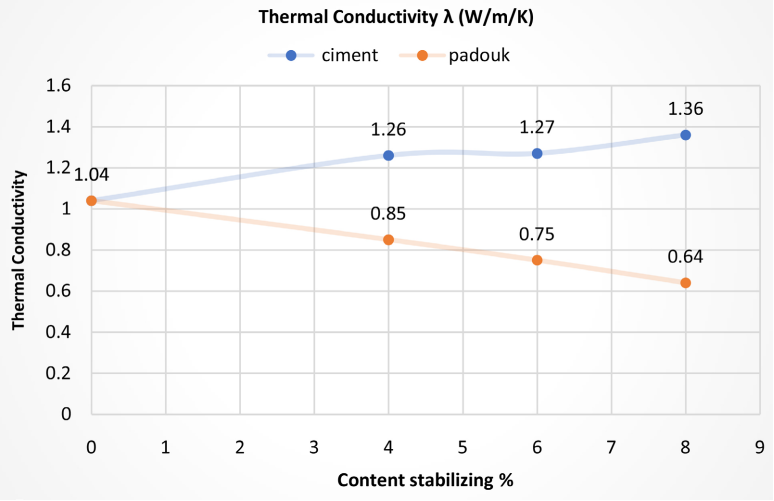

Figure 12. Evolution of thermal conductivity as a function of cement content and padauk sawdust content at different percentages (0%, 4%, 6%, 8%).

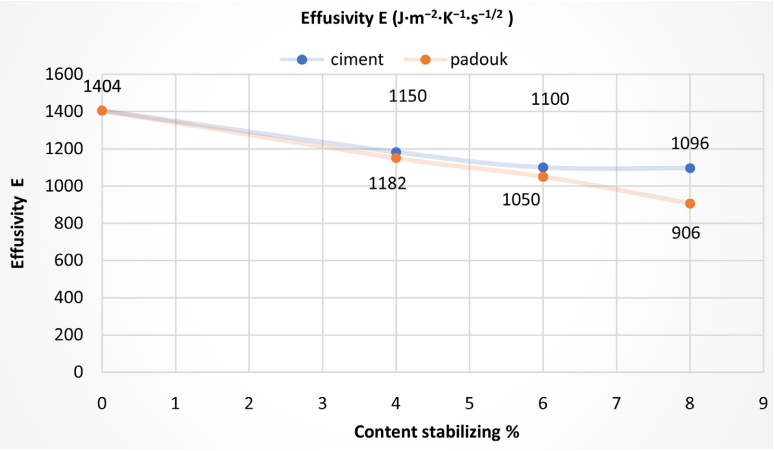

Figure 13. Evolution of effusivity as a function of cement content and padauk sawdust content at different percentages (0%, 4%, 6%, 8%).

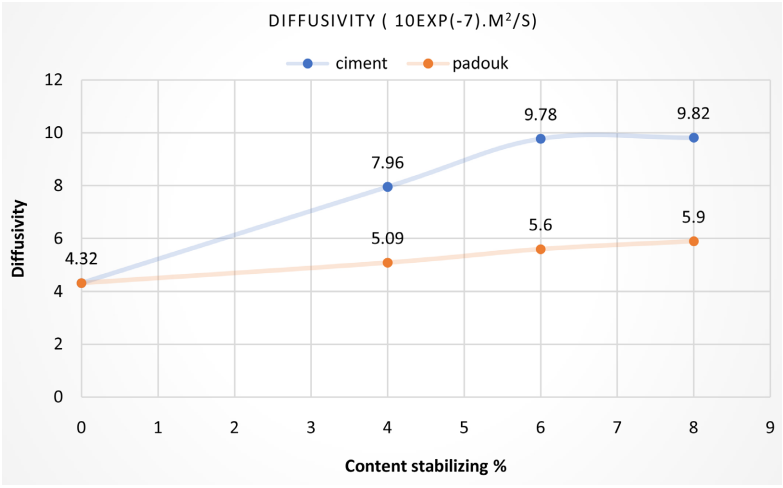

Figure 14. Evolution of diffusivity as a function of cement content and sawdust content at different percentages (0%, 4%, 6%, 8%).

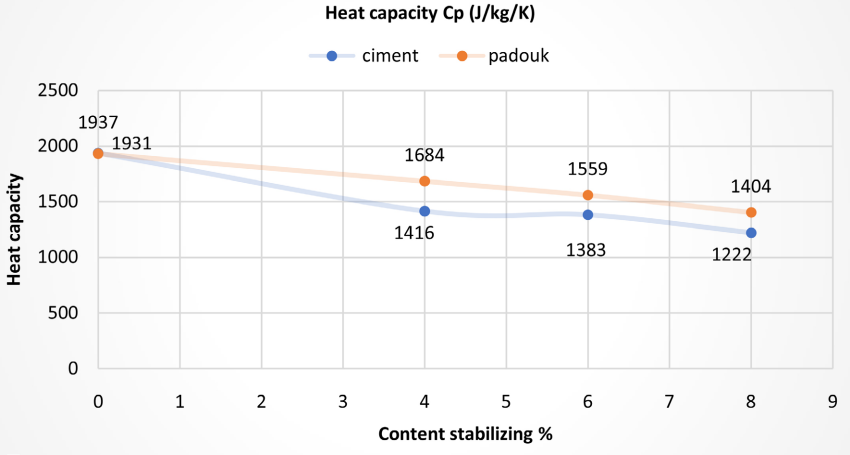

Figure 15. Evolution of heat capacity as a function of cement content and sawdust content at different percentages (0%, 4%, 6%, 8%).

5. Results Analysis

We determined the thermal conductivity, thermal diffusivity, thermal effusively, and heat capacity of our materials experimentally using the asymmetric hot-plane method.

In general, we found that the properties of earthen materials vary with the addition of stabilisers. The curve obtained from **Figure 12** shows that the thermal conductivity varies with the cement and sawdust content. There is an increase in conductivity with the addition of cement and a decrease with the addition of sawdust.

From 1048 W/(m·K) for blocks without stabiliser, the value changes to 12,696 W/(m·K) at a cement content of 4% and decreases slightly to 6% while remaining above the control sample, which is 1048 W/(m·K) with 0% cement and sawdust, reaching a maximum value of 13,624 W/(m·K) at a cement content of 8%. When stabilised with sawdust, a decrease in conductivity is observed with the addition of sawdust, and it reaches its minimum value at a sawdust content of 8%, *i.e.*, a value of 0.6485 W/(m·K). The thermal conductivity of a material depends on several parameters [26], such as the nature of the constituents of the material, the water content, the temperature, and the porosity [27]. The decrease in thermal conductivity could be related to an increase in the number of pores or to an increase in the diameter of the pores caused by a poor distribution of the cement [28]. In fact, it is estimated that for this interval, the amount of cement is insufficient to promote the formation of a homogeneous structure [29]. As for the increase in thermal conductivity above 4% cement, it can be caused by an increase in cohesion at the level of the different components of the block [22]. In fact, the hydration of the cement allows the formation of compounds (CSH and portlandite) that strengthen the bonds between the constituents (clay and sand), thus favouring a reduction in porosity (either in quantity or in size), resulting in the creation of a continuous and homogeneous internal structure. This structure is therefore favourable to heat transfer [3] [30] [31]. This explains the increase in

thermal conductivity. It should be noted, however, that the increase in thermal conductivity associated with cement remains close to the thermal conductivity of the block without cement. In fact, the results obtained show that with 6% cement, the thermal conductivity is 1.1576 W/(m·K), a value very close to that obtained for the block without cement (1.048 W/(m·K)). It would therefore be necessary to add more than 8% cement to obtain a thermal conductivity higher than that of the block without cement.

5.1. Comparative Study of Our Conductivities with Some References from the Literature

In the literature, many authors have evaluated the thermal properties of compressed and stabilised earth blocks (Table 3):

Table 3. Comparative study of our conductivities.

Reference (s)	Binders/Fibres	Binder/Fibre Proportion (%)	Method	Initially Stabilised/Control Sample Thermal Conductivity (W/m/K)	Post-Stabilisation Minimum Thermal Conductivity (W/m/K)
In this work	Cement	0	Asymmetrical Hot-Plane Method	1.04	1.04
In this work	Cement	4	Asymmetrical Hot-Plane Method	1.04	1.26
In this work	Cement	6	Asymmetrical Hot-Plane Method	1.04	1.27
In this work	Cement	8	Asymmetrical Hot-Plane Method	1.04	1.36
In this work	sawdust content	4	Asymmetrical Hot-Plane Method	1.04	0.85
In this work	sawdust content	6	Asymmetrical Hot-Plane Method	1.04	0.75
In this work	sawdust content	8	Asymmetrical Hot-Plane Method	1.04	0.64
[32]	1.2% Kenaf Fibres	Fibre Length 10 - 40 Mm	Hot-Film Method	2	0.95
[33]	10% Lime + Untreated Date Palm Fibre 10% Lime + Alkali Treated Date Palm Fibre	0 - 0.2	Transient Hot-Wire Method	0.824 0.837	0.761 0.805
[34]	10% Lime + 1% Aloe Vera Mucilage + Coconut Fibre	0 - 0.5	Linear Source of Transient Heat	0.41775	0.35975
[35]	Cement Natural Rubber Latex	8 1 - 5	Hot Disk Method	1	0.96
[36]	Bottom Biomass Ash	0 - 20	Hot Disk Transient Plane Source Method	0.86	0.78
[30]	Metakaolin and Sodium Hydroxide Solution	5 - 20	Asymmetric Hot Plane Method	0.6	0.71

5.2. Comparative Analysis of Additional Thermal Properties

For bricks stabilised with sawdust, the thermal conductivities range from 1.04 W/m/K to 0.64 W/m/K. These values are close to those obtained for the thermal conductivities of CCR-stabilized earth blocks and fibres (Table 4) as reported in [37], which range from 1.02 W/m/K to 0.84 W/m/K. Bricks stabilised with sawdust are classified as insulating materials due to their relatively low conductivity values. This characteristic results in a slowdown of heat transfer and heat flow within the materials. These low values can be attributed to the high porosity levels of the blocks, as the pores contain air, which is a good insulator. The specific heat capacity of the cement-stabilised brick is higher than that of the sawdust-stabilised brick. Therefore, cement-stabilised brick will have a greater heat storage capacity than sawdust-stabilised brick.

Thermal diffusivity values are 4.32×10^{-7} m²/s for unstabilised bricks, ranging from 4.32×10^{-7} m²/s to 5.90×10^{-7} m²/s for bricks stabilised with sawdust and from 4.32×10^{-7} m²/s to 9.82×10^{-7} m²/s for bricks stabilised with cement. These values are consistent with the findings of study [37]. The low values are attributable to the insulation properties of these materials. Heat flow through walls constructed with these bricks, particularly those stabilised with sawdust, will take a considerable amount of time. Diffusivity is a measure of the material's ability to transfer heat.

Table 4. Comparative analysis of additional thermal properties.

Reference(s)	Binders/Fibbers	%	Effusivity, E (J/m²·K·s$^{-1/2}$)	Capacity, C_p (J/kg/K)	Conductivity, λ (W/m/K)	Diffusivity, a (m²/s)
In this work	Cement	0	1404	1937	1.04	4.32×10^{-7}
In this work	Cement	4	1182	1416	1.26	7.96×10^{-7}
In this work	Cement	6	1100	1383	1.27	9.78×10^{-7}
In this work	Cement	8	1096	1222	1.36	9.82×10^{-7}
In this work	Sawdust	4	1150	1684	0.85	5.09×10^{-7}
In this work	Sawdust	6	1050	1559	0.75	5.60×10^{-7}
In this work	Sawdust	8	906	1404	0.64	5.90×10^{-7}
[37]	CCR	0	1291	899	1.02	6.30×10^{-7}
[37]	CCR	5	1152	922	0.89	5.60×10^{-7}
[37]	CCR	10	1159	916	0.84	5.40×10^{-7}
[37]	Cement	8	1231	844	1.01	6.80×10^{-7}
[37]	Fibre	2	1159	916	0.84	5.40×10^{-7}
[37]	Fibre	4	1080	908	0.76	5.00×10^{-7}
[37]	Fibre	8	1055	812	0.83	6.10×10^{-7}

CCR: Calcium Carbide Residue.

The thermal effusivity value for the unstabilised brick is 1404 ($J/m^2 \cdot K \cdot s^{-1/2}$). The values for the cement-stabilised bricks are, respectively, 1182 ($J/m^2 \cdot K \cdot s^{-1/2}$), 1100 ($J/m^2 \cdot K \cdot s^{-1/2}$), and 1096 ($J/m^2 \cdot K \cdot s^{-1/2}$) for cement percentages of 4%, 6%, and 8%. The effusivity values for the sawdust stabilised bricks are, respectively, 1150 ($J/m^2 \cdot K \cdot s^{-1/2}$), 1050 ($J/m^2 \cdot K \cdot s^{-1/2}$), and 906 ($J/m^2 \cdot K \cdot s^{-1/2}$) for sawdust percentages of 4%, 6%, and 8%. The high effusivity values result in bricks quickly absorbing a significant amount of energy without noticeable surface heating.

5.3. Analysis of Reduced Sensitivities to Temperature

The estimation of a parameter is only possible if its reduced sensitivity is non-zero and if all other examined parameters have a zero or constant reduced sensitivity.

The principle of reduced sensitivity analysis has been described by several authors [25]. The reduced temperature sensitivity with respect to a parameter is calculated by

$$k_i \frac{\partial T}{\partial k_i} \tag{31}$$

In practice, the sensitivity of T to the parameter x is calculated as follows:

$$x\frac{\partial T}{\partial x} = x\frac{T(x) - T(1.001x)}{0.001x} = 1000\left[T(x) - T(1.001x)\right] \tag{33}$$

Figure 16 shows the reduced sensitivities of the temperature at the centre of the probe to the parameters E, R_c, and ρc. It can be seen that the temperature at the centre of the probe is at all times significantly sensitive to the effusivity E of the material. Moreover, this sensitivity is not correlated with that of the other parameters. We also note that the temperature is not sensitive to the volumetric heat capacity of the sample at the beginning (up to a time t_1 = 150 s in this case). A simultaneous estimation of the parameters E and ρc from the full model is possible if the estimation time is greater than t1 but within the limits of the unidirectional transfer hypothesis.

5.4. Residual Analysis

Residual curves show the difference between experimental and theoretical data. When residuals are zero (curves at the centre value of zero) within a specified interval, the theoretical and experimental findings are in agreement. Residual curve analysis supports the choice of estimation duration. They can also verify the validity of the hypotheses of unidirectional transfer and the semi-infinite medium.

The residues curve in Figure 17 indicates that the experimental and simulated curves perfectly overlap, indicating that the complete model minimises the sum of quadratic deviations between the two curves. The residues are not signed. The residues are entirely flat throughout the estimated duration. This suggests that accurate thermal parameter estimation can be achieved over the 0 to 500 s time interval.

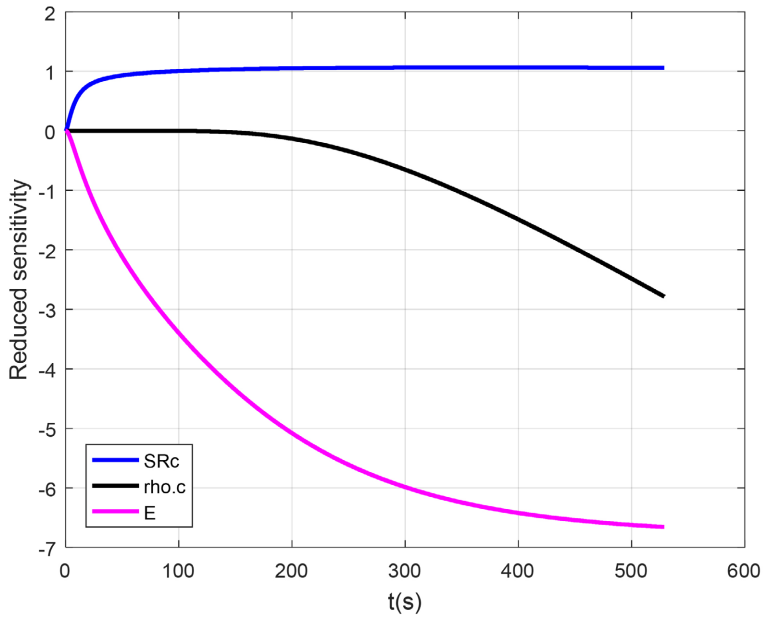

Figure 16. Reduced sensitivity to parameters.

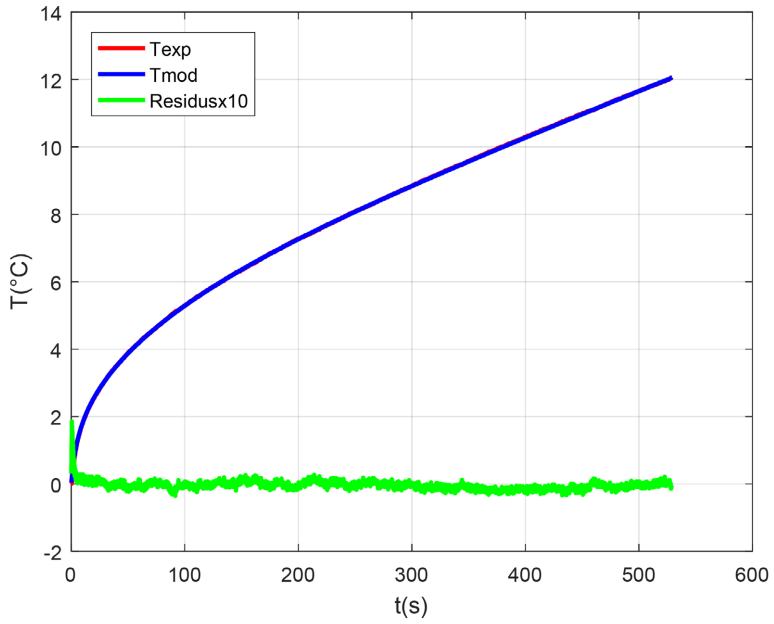

Figure 17. Estimation residuals.

The Levenberg-Marquart algorithm minimises errors between experimental and simulated temperatures. Figure 18 indicates that the results have converged. The perfect overlap of the two curves demonstrates the successful minimisation of differences between the model and the experiment.

In Figure 19, a manifestation of three-dimensional effects during the sample test can be observed. The residues remain perfectly flat until 400 s; a detachment is then observed. This change indicates that the heat transfer is no longer centred and that the convection phenomenon has started. An accurate estimate of the

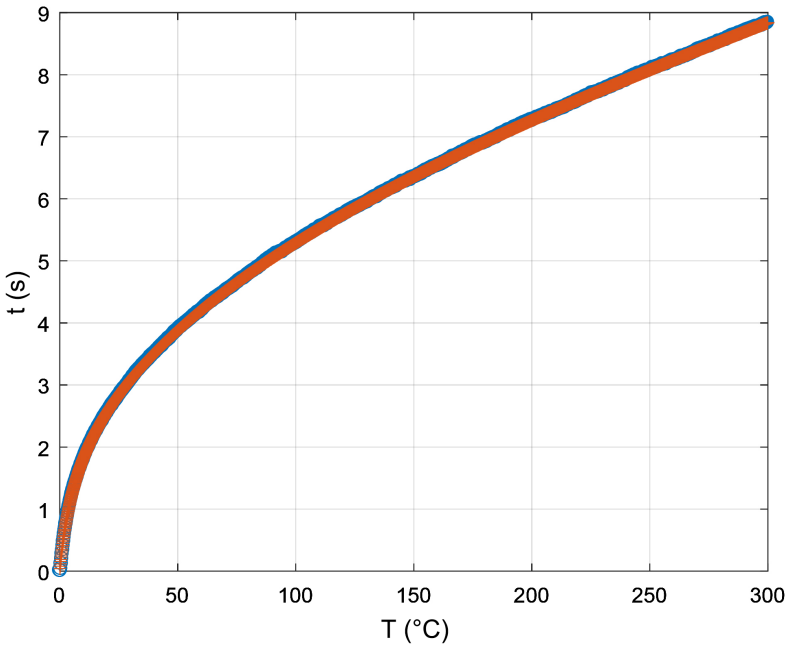

Figure 18. Covariance.

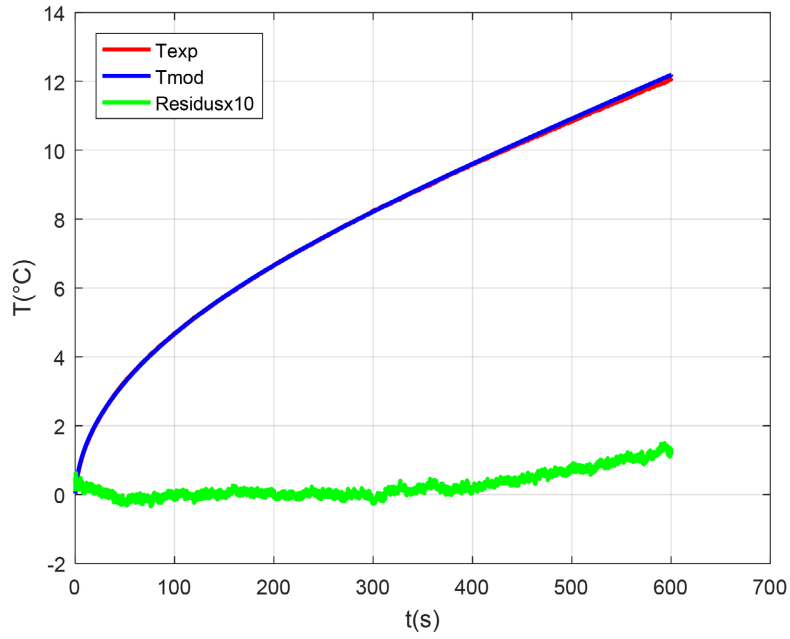

Figure 19. Residuals at parameters.

sample's thermophysical parameters should be made between 100 and 300 s. This observation is generalisable to much longer periods. It has been observed that the densest materials demonstrate less sensitivity to heat flow.

During data collection, the experimental curve and the theoretical curve may converge relatively, but the residues may not be centred at the end. Possible causes of this phenomenon are the low quality of the energy source, a defect in the specimen's dimensioning, or an unevenness in the specimen's surface.

5.5. Application of the Work

This work, which is part of the theme of sustainable development, is applied in various sectors. In the field of recycling, it shows a way of valorising sawdust, which is very often used only as firewood. It also contributes to the fight against global warming, as we show that the stabilisation of blocks of earth with agricultural residues can be used as a substitute for cement, thus reducing the emission of greenhouse gases. Understanding the properties of materials helps engineers to better design homes by facilitating the assessment of thermal comfort.

6. Conclusions

From the results, it is clear that with the right approach to stabilisation, it is possible to manufacture different types of bricks that have better physical, mechanical, and thermal properties (thermal conductivity, diffusivity, and effusivity) than others depending on the different stabilisers.

The behaviour of the material varies depending on the stabiliser used. Studies have demonstrated that stabilisation with plant fibres enhances the mechanical and thermal properties of earth blocks.

Please note that the search for appropriate properties varies depending on the application or climate of the construction area. For instance, the search for the appropriate material behaviour in the hot climate of northern Cameroon would differ from the search for such behaviour in material for western Cameroon, with a cold climate. As previously mentioned, this research aims to enhance the thermal comfort of buildings by promoting the development of high-quality materials. The materials used in this research include earth, cement, and sawdust, which have historically been undervalued and often burned. Mud bricks are significantly affected by structural and chemical changes resulting from cement hydration and the presence of sawdust.

The study shows that stabilising earth bricks with cement or sawdust improve the thermal behaviour of the material, thus increasing the building's thermal comfort. However, the search for specific properties is dependent on the field of application or use. The asymmetric hot-plane method used for thermal characterisation seems to be a reliable, easy-to-implement, and inexpensive way to determine the thermal properties of a material.

Our findings align with those of other researchers who have studied the thermal properties of stabilised earth bricks. Any distinctions between our research and existing literature can be attributed to the unique composition of our materials and the physicochemical properties of the raw earth material. Nevertheless, our findings are consistent with the existing literature.

- We have demonstrated that stabilising earth bricks with cement contribute to the enhancement of their thermal conductivity.
- In this study, we demonstrated that stabilising earth bricks with padauk sawdust reduce thermal conductivity. On the other hand, stabilising with cement increases thermal conductivity.

- We discovered that stabilising earth bricks with sawdust decrease the thermal properties such as diffusivity, effusivity, and calorific capacity. This is not the case when cement is used for stabilisation.

We demonstrate that sawdust, which is often burned and not valued in Cameroon, can be utilised in housing. This application falls under the category of biosourced materials that contribute to the thermal comfort of the living environment.

Author Contributions

Validation, N. M. M.; Resources, N. G. A.; Supervision, N. G. E. and D. B. All authors have read and agreed to the published version of the manuscript.

Funding

This research received no external funding.

Data Availability Statement

Not applicable.

Conflicts of Interest

The authors declare no conflict of interest.

References

[1] Kariyawasam, K.K.G.K.D. and Jayasinghe, K. (2016) Cement Stabilized Rammed Earth as a Sustainable Construction Material. *Construction and Building Materials*, **105**, 519-527. https://doi.org/10.1016/j.conbuildmat.2015.12.189

[2] Zhang, L., Gustavsen, A., Jelle, B.P., Yang, L., Gao, T. and Wang, Y. (2017) Thermal Conductivity of Cement Stabilized Earth Blocks. *Construction and Building Materials*, **151**, 504-511. https://doi.org/10.1016/j.conbuildmat.2017.06.047

[3] Toure, P.M., Sambou, V., Faye, M., Thiam, A., Adj, M. and Azilinon, M. (2017) Mechanical and Hygrothermal Properties of Compressed Stabilized Earth Bricks (CSEB). *Journal of Building Engineering*, **13**, 266-271. https://doi.org/10.1016/j.jobe.2017.08.012

[4] Sekhar, D.C. and Nayak, S. (2018) Utilization of Granulated Blast Furnace Slag and Cement in the Manufacture of Compressed Stabilized Earth Blocks. *Construction and Building Materials*, **166**, 531-536. https://doi.org/10.1016/j.conbuildmat.2018.01.125

[5] Ruiz, G., Zhang, X., Edris, W.F., Cañas, I. and Garijo, L. (2018) A Comprehensive Study of Mechanical Properties of Compressed Earth Blocks. *Construction and Building Materials*, **176**, 566-572. https://doi.org/10.1016/j.conbuildmat.2018.05.077

[6] Inim, I.J., Affiah, U.E. and Eminue, O.O. (2018) Assessment of Bamboo Leaf Ash/Lime-Stabilized Lateritic Soils as Construction Materials. *Innovative Infrastructure Solutions*, **3**, Article No. 32. https://doi.org/10.1007/s41062-018-0134-7

[7] Goutsaya, J., Ntamack, G.E. and d'Ouazzane, S.C. (2022) Damage Modelling of Compressed Earth Blocks Stabilised with Cement. *Advances in Civil Engineering*, **2022**, Article ID: 3342661. https://doi.org/10.1155/2022/3342661

[8] Walker, P.J. (2004) Strength and Erosion Characteristics of Earth Blocks and Earth Block Masonry. *Journal of Materials in Civil Engineering*, **16**, 497-506. https://doi.org/10.1061/(ASCE)0899-1561(2004)16:5(497)

[9] Adamski, M. (2003) Polyoptimization of the Form of a Building on an Oval Base. *Archives of Civil and Mechanical Engineering*, **49**, 511-530. https://www.scopus.com/inward/record.uri?eid=2-s2.0-33751533580&partnerID=40&md5=fc4f4a3cad2289344f6f1e005f86a022

[10] Zhelykh, V., Ulewicz, M., Furdas, Y., Adamski, M. and Rebman, M. (2022) Investigation of Pressure Coefficient Distribution on the Surface of a Modular Building. *Energies*, **15**, Article 4644. https://doi.org/10.3390/en15134644

[11] Kapalo, P. and Adamski, M. (2021) The Analysis of Heat Consumption in the Selected City. *Lecture Notes in Civil Engineering*, **100**, 158-165. https://www.scopus.com/inward/record.uri?eid=2-s2.0-85090047428&doi=10.1007%2f978-3-030-57340-9_20&partnerID=40&md5=375a50395472c450e5ebf154a47d6acd

[12] McGregor, F., Heath, A., Fodde, E. and Shea, A. (2014) Conditions Affecting the Moisture Buffering Measurement Performed on Compressed Earth Blocks. *Building and Environment*, **75**, 11-18. https://doi.org/10.1016/j.buildenv.2014.01.009

[13] Danso, H. (2016) Influence of Compacting Rate on the Properties of Compressed Earth Blocks. *Advances in Materials Science and Engineering*, **2016**, Article ID: 8780368. https://doi.org/10.1155/2016/8780368

[14] Bruno, A.W., Gallipoli, D., Perlot, C. and Mendes, J. (2017) Mechanical Behaviour of Hypercompacted Earth for Building Construction. *Materials and Structures*, **50**, Article No. 160. https://doi.org/10.1617/s11527-017-1027-5

[15] Taallah, B., Guettala, A., Guettala, S. and Kriker, A. (2014) Mechanical Properties and Hygroscopicity Behavior of Compressed Earth Block Filled by Date Palm Fibers. *Construction and Building Materials*, **59**, 161-168. https://doi.org/10.1016/j.conbuildmat.2014.02.058

[16] Laborel-Préneron, A., Aubert, J.E., Magniont, C., Tribout, C. and Bertron, A. (2016) Plant Aggregates and Fibers in Earth Construction Materials: A Review. *Construction and Building Materials*, **111**, 719-734. https://doi.org/10.1016/j.conbuildmat.2016.02.119

[17] Bruno, A.W., Gallipoli, D., Perlot, C. and Mendes, J. (2017) Effect of Stabilisation on Mechanical Properties, Moisture Buffering and Water Durability of Hypercompacted Earth. *Construction and Building Materials*, **149**, 733-740. https://doi.org/10.1016/j.conbuildmat.2017.05.182

[18] Arrigoni, A., Beckett, C., Ciancio, D. and Dotelli, G. (2017) Life Cycle Analysis of Environmental Impact vs. Durability of Stabilised Rammed Earth. *Construction and Building Materials*, **142**, 128-136. https://doi.org/10.1016/j.conbuildmat.2017.03.066

[19] Van Damme, H. and Houben, H. (2018) Earth Concrete. Stabilization Revisited. *Cement and Concrete Research*, **114**, 90-102. https://doi.org/10.1016/j.cemconres.2017.02.035

[20] Nshimiyimana, P., Messan, A., Zhao, Z. and Courard, L. (2019) Chemico-Microstructural Changes in Earthen Building Materials Containing Calcium Carbide Residue and Rice Husk Ash. *Construction and Building Materials*, **216**, 622-631. https://doi.org/10.1016/j.conbuildmat.2019.05.037

[21] Izemmouren, O., Guettala, A. and Guettala, S. (2015) Mechanical Properties and Durability of Lime and Natural Pozzolana Stabilized Steam-Cured Compressed Earth Block Bricks. *Geotechnical and Geological Engineering*, **33**, 1321-1333.

https://doi.org/10.1007/s10706-015-9904-6

[22] Nshimiyimana, P., Miraucourt, D., Messan, A. and Courard, L. (2018) Calcium Carbide Residue and Rice Husk Ash for improving the Compressive Strength of Compressed Earth Blocks. *MRS Advances*, **3**, 2009-2014. https://doi.org/10.1557/adv.2018.147

[23] Muntohar, A.S. (2011) Engineering Characteristics of the Compressed-Stabilized Earth Brick. Construction and Building Materials, **25**, 4215-4220. https://doi.org/10.1016/j.conbuildmat.2011.04.061

[24] Jannot, Y., Degiovanni, A., Félix, V. and Bal, H. (2011) Measurement of the Thermal Conductivity of Thin Insulating Anisotropic Material with a Stationary Hot Strip Method. *Measurement Science and Technology*, **22**, Article ID: 035705. https://doi.org/10.1088/0957-0233/22/3/035705

[25] Meukam, P. (2004) Valorisation des briques de terre stabilises en vue de losolation thermique du bâtiment. Ph.D. Thesis, Université de Yaoundé I, Yaoundé.

[26] Houben, H. and Guillaud, H. (2006) Traité de Construction en Terre. Parenthèse, Marseille.

[27] Minke, G. (2006) Building with Earth: Design and Technology of a Sustainable Architecture. Birkhäuser, Basel.

[28] Delgado, M.C.J. and Guerrero, I.C. (2007) The Selection of Soils for Unstabilised Earth Building: A Normative Review. *Construction and Building Materials*, **21**, 237-251. https://doi.org/10.1016/j.conbuildmat.2005.08.006

[29] Muthadhi, A. and Kothandaraman, S. (2010) Optimum Production Conditions for Reactive Rice Husk Ash. *Materials and Structures*, **43**, 1303-1315. https://doi.org/10.1617/s11527-010-9581-0

[30] Sore, O.S., Messan, A., Prud'Homme, E., Escadeillas, G. and Tsobnang, F. (2018) Stabilization of Compressed Earth Blocks (CEBs) by Geopolymer Binder Based on Local Materials from Burkina Faso. *Construction and Building Materials*, **165**, 333-345. https://doi.org/10.1016/j.conbuildmat.2018.01.051

[31] Mansour, M.B., Jelidi, A., Cherif, A.S. and Jabrallah, S.B. (2016) Optimizing Thermal and Mechanical Performance of Compressed Earth Blocks (CEB). *Construction and Building Materials*, **104**, 44-51. https://doi.org/10.1016/j.conbuildmat.2015.12.024

[32] Laibi, A.B., Poullain, P., Leklou, N., Gomina, M. and Sohounhloué, D.K. (2018) Influence of the Kenaf Fiber Length on the Mechanical and Thermal Properties of Compressed Earth Blocks (CEB). *KSCE Journal of Civil Engineering*, **22**, 785-793. https://doi.org/10.1007/s12205-017-1968-9

[33] Taallah, B. and Guettala, A. (2016) The Mechanical and Physical Properties of Compressed Earth Block Stabilized with Lime and Filled with Untreated and Alkali-Treated Date Palm Fibers. *Construction and Building Materials*, **104**, 52-62. https://doi.org/10.1016/j.conbuildmat.2015.12.007

[34] Velasco-Aquino, A.A., Espuna-Mujica, J.A., Perez-Sanchez, J.F., Zuñiga-Leal, C., Palacio-Perez, A. and Suarez-Dominguez, E.J. (2021) Compressed Earth Block Reinforced with Coconut Fibers and Stabilized with Aloe Vera and Lime. *Journal of Engineering, Design and Technology*, **19**, 795-807. https://doi.org/10.1108/JEDT-02-2020-0055

[35] Jose, A. and Kasthurba, A.K. (2021) Laterite Soil-Cement Blocks Modified Using Natural Rubber Latex: Assessment of Its Properties and Performance. *Construction and Building Materials*, **273**, Article ID: 121991. https://doi.org/10.1016/j.conbuildmat.2020.121991

[36] Muñoz, P., Letelier, V., Muñoz, L. and Zamora, D. (2021) Assessment of Technological Performance of Extruded Earth Block by Adding Bottom Biomass Ashes. *Journal of Building Engineering*, **39**, Article ID: 102278. https://doi.org/10.1016/j.jobe.2021.102278

[37] Philbert, N. (2020) Effect of the Type of Clay Earthen Materials and Substitution Materials on the Physico-Mechanical Properties and Durability of Compressed Earth Blocks. Ph.D. Thesis, Université de Liège, Liege.